Chinese Chemical Letters 32 (2021) 3421–3425

Contents lists available at ScienceDirect

Chinese Chemical Letters

journal homepage: www.elsevier.com/locate/cclet

Communication

Dual-readout test strips platform for portable and highly sensitive detection of alkaline phosphatase in human serum samples

Juanzu Liu, Hongmin Meng, Lin Zhang*, Shasha Li, Juan Chen, Yi Zhang*, Jianjun Li, Lingbo Qu, Zhaohui Li*

Institute of Chemical Biology and Clinical Application at the First Affiliated Hospital, Zhengzhou Key Laboratory of Functional Nanomaterial and Medical Theranostic, College of Chemistry, Zhengzhou University, Zhengzhou 450001, China

ARTICLE INFO

Article history:
Received 9 February 2021
Revised 12 March 2021
Accepted 12 May 2021
Available online 21 May 2021

Keywords:
Lateral flow test strip
MnO_2 nanosheets
Quantum dots
Dual-readout
Alkaline phosphatase

ABSTRACT

In this work, a very simple dual-readout lateral flow test strip (LFTS) platform was developed for sensitive detection of alkaline phosphatase (ALP) based on a portable device. In this assay, quantum dots (QDs) conjugated with bovine serum albumin (QDs-BSA) were chosen as fluorescence signal labels. In the absence of ALP, MnO_2 nanosheets aggregate on the test line and exhibit an obvious brown color, which can be observed by naked eyes to realize semi-qualitative analysis. Meanwhile, fluorescence intensity of QDs-BSA can also be effectively quenched by MnO_2 nanosheets due to inner-filter effect. Correspondingly, in the presence of ALP, ALP can catalyze the hydrolysis of ascorbic acid 2-phosphate (AAP) to generate L-ascorbic acid (AA), which can reduce MnO_2 into Mn^{2+}, accompanying with the obvious fluorescence recovery of the QDs. By simply monitoring the change of colorimetric and fluorescent signal on the test line, trace amount of ALP can be quantitatively detected. Under the optimal conditions, measurable evaluation of ALP was reached in a linear range from 1 U/L to 20 U/L with a detection limit of 0.7 U/L based on fluorescence signal. Furthermore, this colorimetric/fluorescent dual-readout assay was successfully applied to monitor ALP in human serum samples, showing its great potential as a point of care biosensor for clinical diagnosis.

Alkaline phosphatase (ALP), an essential and universal hydrolase in human body, plays a vital role in normal growth of organism [1–3]. Moreover, this enzyme can catalyze hydrolysis of phosphoryl esters and has been used as a crucial clinical diagnosis indicator for the variety of diseases [4–6]. The expression levels of ALP in different organisms are not uniform, ranging from 46 U/L to 190 U/L in adult serum and above 500 U/L in children and pregnant women [7]. The concentration of ALP deviation is associated with many diseases, such as bone disorders (osteoporosis and bone tumor), hepatobiliary and liver dysfunction (extrahepatic biliary tract obstruction,cirrhosis and hepatitis), breast and prostatic cancer, and diabetes mellitus [8–10]. Thus, convenient and sensitive quantification of ALP level in complex biological systems is highly meaningful.

To date, many analytical methods for ALP determination have been developed, such as chemiluminescence [11,12], electrochemistry [13], colorimetry [14,15], chromatographic and surface enhancement Raman scattering assay [16,17]. Despite these techniques are useful and have been successfully applied to sensing ALP, most of them still have some hindrances including high cost and specialized equipment, time-consuming and difficulties connected with implementation in point-of-care clinical diagnostics, which greatly limit their applications. Therefore, exploring novel methods, meeting the demand of simplicity, rapidness, low-cost, high sensitivity and highly accurate on-site diagnosis are still urgently needed.

Recently, lateral flow test strips (LFTSs) have received extensive attention due to their rapidness, robustness, low-cost, and low technical barrier [18–20], Up to now, most of the previously reported LFTS systems were based on single readout, either colorimetric or fluorometric [21–23], which was not convincing enough because many factors may interfere with the signals readout. To obtain better performance for measuring disease indicators or monitoring the efficacy of therapeutic treatment, new LFTS with multiple signals is highly required. Compared with single signal, dual/multiple signals LFTS have higher sensitivity, higher accuracy and wider application range [24,25].

* Corresponding authors.
E-mail addresses: zhanglin@zzu.edu.cn (L. Zhang), zhangyi@zzu.edu.cn (Y. Zhang), zhaohui.li@zzu.edu.cn (Z. Li).

https://doi.org/10.1016/j.cclet.2021.05.019
1001-8417/

Manganese dioxide (MnO_2) nanosheets, as a new kind of 2D nanomaterials, have received great favor by researchers in recent years owing to their excellent physical and chemical properties [26–28]. Based on their broad and intense absorption band and fast electron transfer rate, MnO_2 nanosheets have been widely utilized as fluorescence quencher to fabricate biosensors [29–31]. For example, our group has developed a fluorescence "switch-on" probes for rapid glutathione detection by using carbon dots and MnO_2 nanocomposites [32]. Lin *et al.* also utilized MnO_2 nanosheets-carbon dots for the sensitive detection of organophosphorus pesticides [33]. More interestingly, many previous work show that ALP can catalyze the hydrolysis of ascorbic acid 2-phosphate (AAP) to generate ascorbic acid (AA) [34] and AA can lead to the decomposition of the MnO_2 nanosheets [35–37]. On the basis of this knowledge, MnO_2 nanocomposite may possess great potential for the sensitive detection of ALP.

Herein in this work, a novel dual-readout LFTS for ALP detection was fabricated based on MnO_2 nanosheets and fluorescence quantum dots (QDs). The principle of this dual-readout platform was shown in Scheme 1. In the absence of ALP, MnO_2 nanosheets aggregate on the test line exhibiting a dark brown color to adopt as a colorimetric signal. Meanwhile, the fluorescence intensity of QDs-BSA compound can be quenched by captured MnO_2 nanosheets. In the presence of ALP, ALP can effective bio-catalyze AAP hydrolysis to generate AA, which reduces MnO_2 to Mn^{2+}. As a result, the brown color on the test line fades and the fluorescence signal of QDs also recover. The change of color and fluorescence intensity of QDs is highly depended on the concentration of ALP. More importantly, this new developed dual-readout sensor displays a great potential for detecting ALP with advantages of simplicity, good reproducibility, robust stability and low-cost.

The detailed synthesis process of QDs and QDs-BSA conjugates can be found in Supporting information. And the physicochemical property of QDs and QDs-BSA were characterized by Transmission electron microscopy (TEM), fluorescence emission spectrum, UV-vis spectroscopy and Fourier transform infrared (FT-IR) spectrum. As shown in Fig. S1 (Supporting information), the TEM image (Fig. S1A) shows that QDs are spherical shape and possess a uniform size distribution. The fluorescence emission spectrum (Fig. S1B) displays that the emission peak of BSA and QDs at 450 nm and 615 nm. Meanwhile, QDs-BSA conjugates have obvious emission peaks at 450 nm and 615 nm corresponding to emission peak of BSA and QDs. As shown in Fig. S1D, the FT-IR spectrum of QDs-BSA resembled that of QDs, giving clear evidence that the BSA formed part of the nanocomposite. In the spectrum of QDs-BSA, the peaks at 1647 cm^{-1} and 1652 cm^{-1} were assigned to the asymmetric stretching of C=O, while the peak at 1537 cm^{-1} and 1290 cm^{-1} corresponding to C-N of amide bond. All these characterization results demonstrate that the QDs and QDs-BSA have been prepared successful.

The prepared MnO_2 nanosheets material was characterized by transmission electron microscopy (TEM) and UV-vis spectroscopy to investigate its morphological structure and optical properties. As shown in Fig. S2 (Supporting information), the TEM image shows that MnO_2 nanosheets have an obvious two-dimensional nanosheet structure (Fig. S2A). The UV-vis absorption spectrum of material is illustrated in Fig. S2B, the as-prepared MnO_2 nanosheets exhibit a broad absorption and have an intense absorption peak at around 374 nm. These properties clearly demonstrate that MnO_2 nanosheets was successfully prepared, which laid a solid foundation for all the experiments in this design.

To investigate the feasibility of this dual-readout LFTS, we monitored the change of colorimetric signal and fluorescence signals on test line of dual-readout LFTSs under different experiment conditions (Fig. 1). As shown in Fig. 1B, 5 mmol/L AAP was mixed with PB buffer and then added onto the sample pad of dry LFTSs. A few minutes later, the fluorescence intensity was recorded by a portable fluorescence reader (black curve). When MnO_2 nanosheets were added to the test sample, a weak fluorescence was observed (purple curve), suggesting that MnO_2 nanosheets can efficiently quench the fluorescence of QDs-BSA conjugates. While, when ALP was introduced to the samples, the fluorescence intensity of the test strips was enhanced remarkably (red curve) due to ALP enzymatically hydrolyzed the substrate AAP into AA, which triggered the reduction of MnO_2 nanosheets into Mn^{2+}. Inset in Fig. 1B shows the images of test strips under the daylight lamp and UV lamp in different conditions correspondingly. The experiment results demonstrate that this detection platform can be used to detect ALP with dual-readout signal.

The relevant experimental parameters were carefully optimized to obtain the best analytical performance for ALP sensing. The blocking solution in sample pads, the types and pH of the running buffers and running time all can affect the sensitivity of assay and the activity of ALP. Therefore, we choose the optimum experimental condition. Experimental results showed that 5% sucrose solution as blocking solution, PB buffer with pH 7.4 as running buffer, 10 min for running time can provide the best response for the sensing system (Fig. S3A in Supporting information).

Similarly, the added amount of the MnO_2 nanosheets has a significant influence on the sensitivity of this system. Therefore, the best optimized concentration of MnO_2 nanosheets were investigated. The experiment results were shown in Fig. S4 (Supporting information), the fluorescence intensity of QDs-BSA decreased gradually with the concentration of MnO_2 nanosheets increases. When the MnO_2 nanosheets reached a certain concentration (350 μg/mL), the quenching efficiency slowed down and then reached equilibrium, which suggested that the quenching ability of MnO_2 nanosheets reached the maximum. Thus, the optimum concentration of MnO_2 nanosheets in this assay was chosen as 350 μg/mL. Some relevant photographs of the fluorescent dual-readout LFTS under daylight lamp and UV lamp with different concentrations of MnO_2 nanosheets are shown in Fig. S5 (Supporting information). As shown in Fig. S5A, no test band is observed by the naked eye in the absence of MnO_2 nanosheets. Whereas, a brown band appears on the test line with adding to MnO_2 nanosheets and the color gradually deepens as the amount of MnO_2 nanosheets grows. A strong fluorescence signal can be monitored on the test line (Fig. S5B) without MnO_2 nanosheets. However, the fluorescence signal decreases gradually as the concentrations of MnO_2 nanosheets increases, indicating that this dual-readout LFTS can be successfully used for qualitative and quantitative detection.

In addition, the incubation time of ALP usually has a direct effect on the analytical characteristics of immunoassay. Therefore, the incubation time was also studied and the result was shown in Fig. S6 (Supporting information). With the increase of incubation time, the relative fluorescence intensity significantly increased and then reached equilibrium after 3 min. Therefore, the optimal reaction time after added ALP was chosen as 3 min for further investigation in this assay.

The principle of this dual-readout LFTS is based on AA-mediated specific reduction of the MnO_2 nanosheets to Mn^{2+}. In order to verify whether this assay can be used for ALP detection, the fluorescence signal change of the LFTSs was recorded by a portable reader with addition of different amounts of AA standard samples. As displayed in Fig. 2A, with the increasing concentrations of AA from 0 μmol/L to 700 μmol/L, a dramatic increase of fluorescence intensity on the test line can be observed. Fig. 2B describes the relationship between the fluorescence intensity and the concentrations of AA. These results show that this platform be reliably employed for ALP detection through sensing AA.

It has been proved that ALP can hydrolyze AAP to produce AA at an alkaline environment. Based on this principle, the analytical

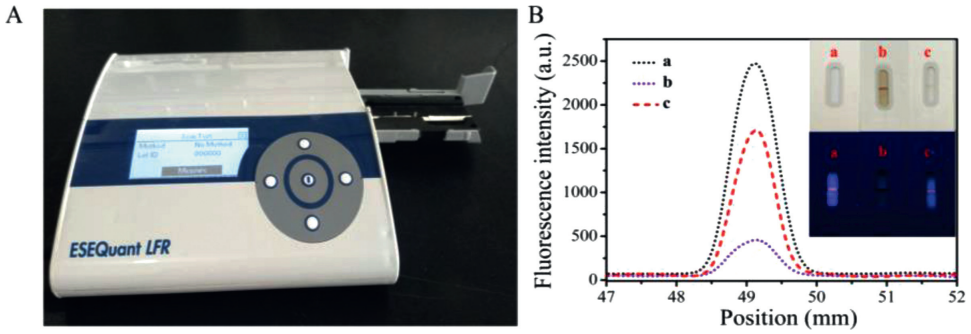

Fig. 1. The feasibility study of the dual-readout LFTS platform. (A) The portable fluorescence reader. (B) Fluorescence signals and images of dual-readout assay for (a) blank sample, (b) add to MnO_2 and AAP, (c) add to MnO_2, AAP and ALP. Inset: Photographs of the dual-readout LFTS with different conditions of a,b,c in daylight lamp and UV lamp, respectively

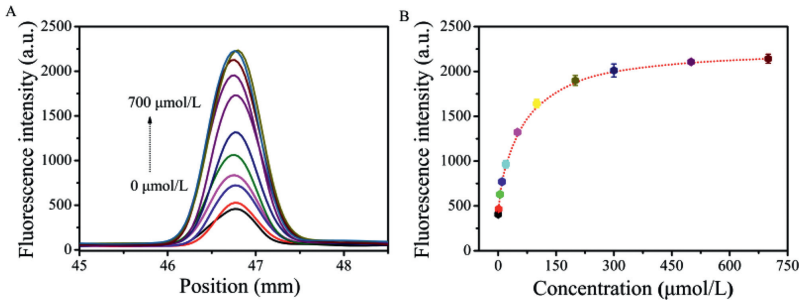

Fig. 2. (A) Fluorescence signals of this dual-readout LFTSs with addition different amounts of AA in a wide range of 0-700 μmol/L (from bottom to top: 0, 1, 5, 10, 20, 50, 100, 200, 300, 500, 700 μmol/L, respectively). (B) Scatter plot of fluorescence intensity as a function of the concentrations of AA (0-700 μmol/L). The error bar represents the standard deviation of parallel experiments.

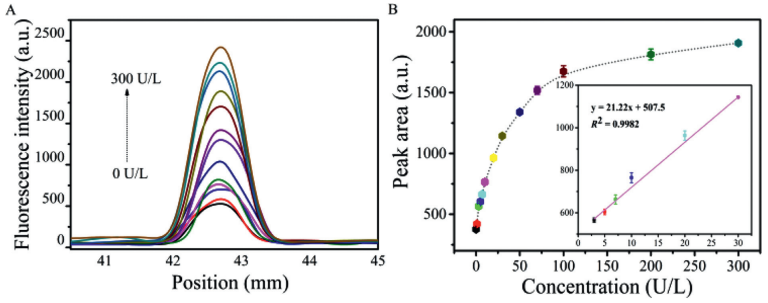

Fig. 3. (A) Fluorescence signals of dual-readout LFTS by addition of ALP with different amount, from bottom to top: 0, 1, 3, 5, 7, 10, 20, 30, 50, 70, 100, 200 and 300 U/L. (B) Scatter plot of fluorescence intensity as a function of the concentrations of ALP (0-300 U/L). Inset: Linear relationship between peak area and the concentration of ALP. The error bar represents the standard deviation of three measurements.

performance of this dual-readout system was first investigated in buffer under the optimal conditions. Fig. 3A shows that the fluorescence intensity on the test line gradually increases with the change of ALP (0-300 U/L) concentration. The calibration curve was obtained by plotting the relationship between fluorescence intensity and ALP concentration (Fig. 3B). Ranging from 1 U/L to 20 U/L, the calibration curve exhibits a good linear relationship (R^2 = 0.9982, inset of Fig. 3B). According to the 3σ/slope calculation, the detection limit for ALP is estimated to be 0.7 U/L. Photos of the LFTSs are shown under the daylight lamp (Fig. S7A in Supporting information) and UV lamp (Fig. S7B in Supporting information) with different amount of ALP. From Fig. S7, we can see that the fluorescence intensity obvious enhance with the increase of ALP concentration, which corresponds to the results from the device readout. As a new type of the test strip, dual/multiple signals LFTS have been used for biomedical monitoring in recent years based on their advantages (Table S1 in Supporting information).

To evaluate the selectivity of dual-readout test strips system for the detection of ALP, some interference substances including bovine serum albumin (BSA), human serum albumin (HSA), glucose oxidase (GOx), immunoglobulin G (IgG), streptavidin (SA), lysozyme (Lys), trypsin (Try), cysteine (Cys), DL-homocysteine (Hcy) and *N*-acetyl-L-cysteine (NAC) were tested. The concentration of ALP is 100 U/L (almost 0.1 nmol/L) [38] and other interference substances are 1 μmol/L, respectively. In Fig. 4A we can see that only ALP can produce a significant fluorescence recovered signal, while other interference substances yield very weak fluorescence responses (F_0 represent the fluorescence intensity of this biosensor in the presence of ALP. Meanwhile, F represents the fluorescence intensity of this dual-readout LFTSs in the presence of other interference substances, respectively). These results demonstrated that our fabricated dual-readout platform has a high specificity to ALP and can be applied for sensing ALP in complex samples.

To evaluate the applicability of this proposed dual-readout test strip in complicated biological systems, the amount of ALP in real human serum samples was performed. The human serum samples were provided by the First Affiliated Hospital of Zhengzhou University (Zhengzhou, China) and obtained from healthy donors. All ex-

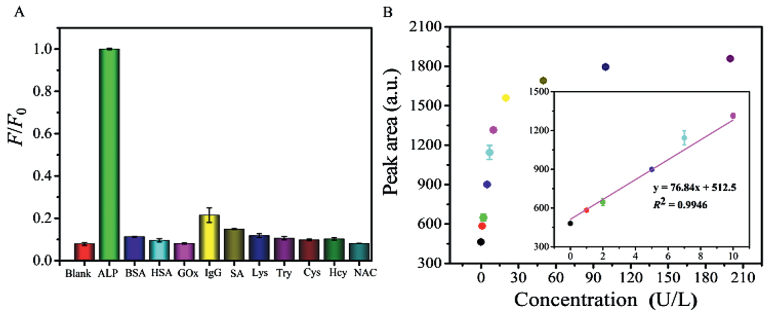

Fig. 4. (A) Investigation of the selectivity of this proposed dual-readout LFTS for ALP detection. The amount of ALP is 100 U/L (almost 0.1 nmol/L) and the amount of other interfering substances are 1 μmol/L. F_0 and F respectively represent the fluorescence intensity in the presence of ALP or other interferences. (B) The fluorescence responses of this dual-readout platform in diluted serum samples to different amount of ALP. Inset: Linear relationship between peak area and the amount of ALP added to the serum.

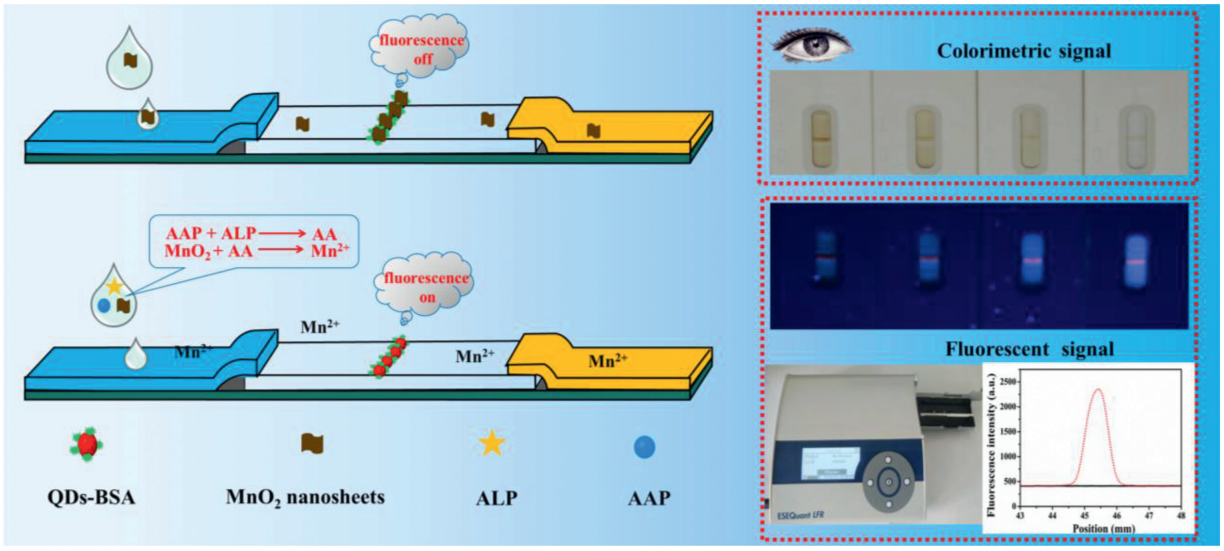

Scheme 1. Schematic illustration of the dual-readout LFTS for detection of ALP.

periments were approved by the Life-Science Ethics Review Committee of Zhengzhou University and obtained the informed consent from the blood donors of this project. The human serum samples were provided by the First Affiliated Hospital of Zhengzhou University (Zhengzhou, China) and obtained from healthy donors. All experiments were approved by the Life-Science Ethics Review Committee of Zhengzhou University and obtained the informed consent from the blood donors of this project. The human serum was diluted 100-fold due to the high level of ALP in the normal serum sample. In Fig. 4B, the fluorescence intensity increases obviously with the change of ALP from 0 U/L to 200 U/L. Meanwhile, a good linear relationship was obtained in complex serum sample in ranging from 1 U/L to 10 U/L. In Fig. S8 (Supporting information) we can see the photos of the LFTSs under the daylight lamp (Fig. S8A) and UV lamp (Fig. S8B) with the addition of different amount of ALP in human serum samples. Obviously, the fluorescence signal recovered with the reduction and decomposition of MnO_2 nanosheets and these results are consistent with the device readout. The recovery assays for diluted serum samples were further carried out to evaluate the accuracy and reliability of the practical application of the dual-readout LFTS. As shown in Table S2 (Supporting information), satisfactory recoveries between 98.8% and 106% are achieved. All results demonstrate that this developed dual-readout test strip has good reliability and can be applied for the practical application for ALP detection in complex mixtures with many advantages including rapidness, portability and cost-effectiveness, *etc*.

In summary, a dual-readout LFTS sensor was developed for sensitively, rapidly and portably detecting ALP based on "off-on" signal switch mechanism. The aggregation of MnO_2 nanosheets effectively quench the system fluorescence based on inner-filter effect of fluorescence. However, in the presence of AA, the fluorescence of QDs can recover because MnO_2 nanosheets are reduced to Mn^{2+}. ALP can bio-catalyze AAP hydrolysis to AA, thus, the quantitative analysis of ALP can be achieved indirectly by monitoring the increase of fluorescence. As well as, the qualitative analysis of ALP can be achieved by analyzing the change of color on the test line *via* naked eyes. This new test strip system may open a new door towards developing various simple, cost-effective, and portable dual-readout fluorescence detection platform in bioassay constructions.

Declaration of competing interest

The authors declare that they have no known competing financial interests or personal relationships that could have appeared to influence the work reported in this paper.

Acknowledgments

This work was supported by the National Natural Science Foundation of China (Nos. 21974125, 21605038), the National 111 Project (No. D20003), the Collaborative Innovation Project of Zhengzhou

(Zhengzhou University) (No. 18XTZX12002), and the Key Scientific Research Project in Universities of Henan Province (No. 19A150048).

Supplementary materials

Supplementary material associated with this article can be found, in the online version, at doi:10.1016/j.cclet.2021.05.019.

References

[1] J. Liang, R.T. Kwok, H.B. Shi, B.Z. Tang, B. Liu, ACS Appl. Mater. Interfaces 5 (2013) 8784–8789.
[2] J.J. Liu, D.S. Tang, Z.T. Chen, et al., Biosens. Bioelectron. 94 (2017) 271–277.
[3] Y.X. Han, J. Chen, Z. Li, H.L. Chen, H.D. Qiu, Biosens. Bioelectron. 148 (2020) 111811.
[4] Z. Li, X.L. Ren, C.X. Hao, X.W. Meng, Z.H. Li, Sens. Actuators B: Chem. 260 (2018) 426–431.
[5] Y. Zeng, J.Q. Ren, S.K. Wang, et al., ACS Appl. Mater. Interfaces 9 (2017) 29547–29553.
[6] Y.Y. Yang, C. Zhang, R.Z. Pan, et al., Chin. Chem. Lett. 31 (2020) 125–128.
[7] H.B. Wang, Y. Li, Y. Chen, Microchim. Acta. 185 (2018) 102.
[8] J.B. Ma, B.C. Yin, X. Wu, B.C. Ye, Anal. Chem. 88 (2016) 9219–9225.
[9] L. Chen, G.C. Yang, P. Wu, C.X. Cai, Biosens. Bioelectron. 96 (2017) 294–299.
[10] Y.L. Hu, X. Geng, L. Zhang, et al., Sci. Rep. 7 (2017) 5849.
[11] H. Jiang, X.M. Wang, Anal. Chem. 84 (2012) 6986–6993.
[12] X.L. Ma, X. Zhang, X.L. Guo, et al., Talanta 154 (2016) 175–182.
[13] J.K. Lee, C.T. Bubar, H.G. Moon, et al., ACS Sens 3 (2018) 2709–2715.
[14] H.P. Jiao, J. Chen, W.Y. Li, et al., ACS Appl. Mater. Interfaces 6 (2014) 1979–1985.
[15] H.W. Song, H.Y. Wang, X. Li, et al., Anal. Chim. Acta 1044 (2018) 154–161.
[16] C.M. Ruan, W. Wang, B.H. Gu, Anal. Chem. 78 (2006) 3379–3384.
[17] A. Ingram, B.D. Moore, D. Graham, Bioorg. Med. Chem. Lett. 19 (2009) 1569–1571.
[18] L.L. Guo, X.L. Wu, L.Q. Liu, H. Kuang, C.L. Xu, Small 14 (2018) 1701782.
[19] C.N. Loynachan, M.R. Thomas, E.R. Gray, et al., ACS Nano 12 (2018) 279–288.
[20] Q.S. You, M.M. Liu, Y. Liu, et al., ACS Sens 2 (2017) 569–575.
[21] J.Z. Liu, J.Y. Wang, Z.H. Li, et al., Microchim. Acta 185 (2018) 110.
[22] Y. Wu, W. Peng, Q. Zhao, et al., Chin. Chem. Lett. 28 (2017) 1881–1884.
[23] J. Hu, Z.L. Zhang, C.Y. Wen, et al., Anal. Chem. 8 (2016) 6577–6584.
[24] T.X. Ji, X.Q. Xu, X.D. Wang, et al., ACS Nano 14 (2020) 16864–16874.
[25] J. Hu, Y.Z. Jiang, M. Tang, et al., Anal. Chem. 91 (2019) 1178–1184.
[26] J. Liu, L.J. Meng, Z.F. Fei, et al., Biosens. Bioelectron. 90 (2017) 69–74.
[27] Y.H. Wang, K. Jiang, J.L. Zhu, L. Zhang, H.W. Lin, Chem. Commun. 51 (2015) 12748–12751.
[28] X. Yan, Y. Song, C.Z. Zhu, et al., ACS Appl. Mater. Interfaces 8 (2016) 21990–21996.
[29] M. Ou, J. Huang, X.H. Yang, et al., Chem. Sci. 8 (2017) 668–673.
[30] K. Kai, Y. Yoshida, H. Kageyama, et al., J. Am. Chem. Soc. 130 (2008) 15938–15943.
[31] H.M. Meng, D. Zhao, N. Li, J.B. Chang, Analyst 143 (2018) 4967–4973.
[32] Q.Y. Cai, J. Li, J. Ge, et al., Biosens. Bioelectron. 72 (2015) 31–36.
[33] X. Yan, Y. Song, C.Z. Zhu, et al., Anal. Chem. 90 (2018) 2618–2624.
[34] L.P. Gao, Z.Z.Huang Y.Li, H.L. Tan, Anal. Chim. Acta 1148 (2021) 238193.
[35] Y.T. Gong, F. Yuan, Y.M. Dong, Z.J. Li, G.L. Wang, Anal. Chim. Acta 1014 (2018) 19–26.
[36] Y.Q. Mei, Q. Hu, B.J. Zhou, et al., Talanta 176 (2018) 52–58.
[37] T. Xiao, J. Sun, J.H. Zhao, et al., ACS Appl. Mater. Interfaces 10 (2018) 6560–6569.
[38] L.L. Zhang, J.J. Zhao, M. Duan, et al., Anal. Chem. 85 (2013) 3797–380.